CrystEngComm

Accepted Manuscript

This is an *Accepted Manuscript*, which has been through the Royal Society of Chemistry peer review process and has been accepted for publication.

Accepted Manuscripts are published online shortly after acceptance, before technical editing, formatting and proof reading. Using this free service, authors can make their results available to the community, in citable form, before we publish the edited article. We will replace this *Accepted Manuscript* with the edited and formatted *Advance Article* as soon as it is available.

You can find more information about *Accepted Manuscripts* in the Information for Authors.

Please note that technical editing may introduce minor changes to the text and/or graphics, which may alter content. The journal's standard Terms & Conditions and the Ethical guidelines still apply. In no event shall the Royal Society of Chemistry be held responsible for any errors or omissions in this *Accepted Manuscript* or any consequences arising from the use of any information it contains.

ROYAL SOCIETY OF CHEMISTRY

www.rsc.org/crystengcomm

Cite this: DOI: 10.1039/c0xx00000x

www.rsc.org/xxxxxx

ARTICLE TYPE

One-step synthesis of highly aligned SnO_2 nanorods on self-produced $Na_2Sn(OH)_6$ substrate for high-performance lithium-ion batteries

Xiguang Han,*[ab] Xiao Han,[a] Linqiang Sun,[a] Qianqian Liu,[a] Wei Xu,[a] Liang Li,[a] Po Wang,[a] Chao Wang[a]

Received (in XXX, XXX) Xth XXXXXXXXX 200X, Accepted Xth XXXXXXXXX 200X

DOI: 10.1039/b000000x

Highly aligned SnO_2 nanorods on self-produced $Na_2Sn(OH)_6$ substrate have been synthesized by one-step hydrothermal synthesis method. The TEM images indicate that the SnO_2 nanorods are exposed with {110} facet. The formation mechanism of the structure has been thoroughly researched by changing the reaction time. The $SnO_2/Na_2Sn(OH)_6$ structure exhibits high-performance of lithium-ion battery.

Lithium-ion batteries have acquired tremendous interest for portable electronic devices in a variety of consumers and medical products because of their high theoretical capacity and long cycle-life.[1,2] However, enhancing the charge/discharge rate capability while maintaining the specific capacity enough high remains a significant challenge.[3-5] Developing high rate capable electrode materials presents an important direction to improve charge/discharge capacity.[4-6] Metal oxides which have high theoretical specific capacity have long been a kind of promising alternative anode materials to graphite (372 mAh g^{-1}).[7-10] Recently, different kinds of metal oxides have been widely exploited as the anode materials in lithium-ion batteries.

Among the various metal oxide materials, SnO_2 has been regarded as a promising material for lithium-ion batteries anodes due to its high theoretical energy capacity (790 mAh g^{-1}).[11-13] However, significant capacity fading with cycling is a problem due to enormous volume changes during Li alloying and dealloying leading to metal segregation and crystallographic deformation.[14-16] To circumvent this problem, several approaches have been proposed for creation of a highly stable SnO_2-based electrode structure. For example, surface modification on the SnO_2 with a second phase,[17,18] changing the morphologies of SnO_2.[19-21] Constructing nanostructure electrode materials has been demonstrated an important way to solve the problem due to their better accommodation of the strains during Li-ion insertion-desertion than in bulk materials.[22-24] Especially, constructing one-dimensional (1D) nanostructure anode arrayed on a substrate is a more effective solution against the volume change problem, because the geometry of nanowires and nanorods is not easily pulverized or broken due to facile strain relaxation.[25-32] For example, Liu and co-workers synthesized SnO_2 nanorod arrays on metallic substrates and demonstrated as a high-performace anode material for lithium ion batteries.[28] Qi et al. fabricated the mesocrystalline SnO_2 nanorods on arbitrary substrates and exhibited superior rate performance.[29]

Recently, numerous different techniques have been reported to prepare 1D SnO_2 nanostructures including physical or chemical vapor deposition,[32-34] pulsed laser deposition,[35] hydrothermal synthesis,[36] thermal evaporation,[37] and solvothermal method.[38] Mostly, templates are used to grow and pattern the SnO_2 nanostructures. For example, zheng and coworkers fabricated SnO_2 nanowire arrays based on a highly-ordered nanoporous alumina membrane (AAM).[39] Wu et al. synthesized arrays of nanoporous tin oxide nanorods by electrodepositing of tin into anodic aluminum oxide (AAO).[40] Hydrothermal synthesis has been applied as an effective template-free method to synthesize the 1D array structure. However, most of the synthesis of array structures by hydrothermal synthesis requires addition of some materials as the substrates. For example, Guo and co-workers synthesis of SnO_2 nanoflower arrays using indium tin oxide (ITO) glass as the substrate by hydrothermal synthesis.[41] Xue et al. fabricated Co_3O_4 nanoneedle arrays on copper foil substrate via hydrothermal synthesis.[42] According to our knowledge, well-aligned SnO_2 1D nanostructures arrays growing directly on the self-produced have rarely been realized.

In this communication, we synthesized highly aligned SnO_2 nanorods on self-produced $Na_2Sn(OH)_6$ substrate by one-step template-free hydrothermal synthesis method. The formation mechanism of the structure has been thoroughly researched by changing the reaction time. The $SnO_2/Na_2Sn(OH)_6$ (SN) structure exhibits high-performance of lithium-ion batteries.

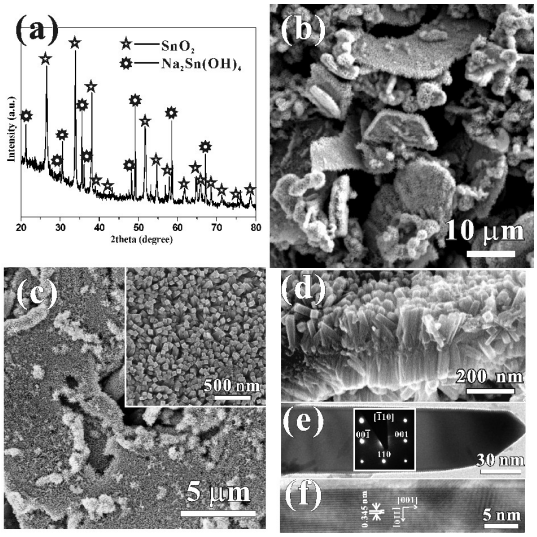

CrystEngComm Accepted Manuscript

Fig. 1 (a) XRD pattern of the SN array (b), (c), SN array at different magnifications, (d) SEM image of SN array viewed from laterally, (e) TEM image of an individual SnO_2 nanorod, insert: the corresponding SAED pattern along the [$\bar{1}$10] axis, (f) the HRTEM image of the SnO_2 nanorod.

The crystal structure and phase purity of the as-prepared products have been characterized by X-ray powder diffraction (XRD) (Fig. 1a). The XRD pattern of the products displays sharp peaks in the 2theta between 20 and 80 degree. The diffraction peaks have been marked by five-pointed star at 26.7, 34.1, 38.1, 39.5, 42.8, 52.2, 54.9, 58.4, 62.3, 65.2, 66.2, 71.4, 79.1 degree corresponding to 110, 101, 200, 111, 210, 211, 220, 002, 310, 112, 301, 202, 321 reflections of the tetragonal rutile SnO_2 (JCPDF: 00-002-1340), and the peaks marked by multi-angle star at 21.4, 30.3, 30.8, 35.9 37.4 degrees correlate to the 012, 110, 104, 113, 202 reflections of $Na_2Sn(OH)_6$ (JCPDF: 00-024-1143). The morphology of the final product has been observed by SEM images (Fig. 1b-d). The low-magnification SEM image in Fig. 1b clearly shows the typical morphology of the as-obtained product, and demonstrates the large scale of the product having rough surface with tens of micrometres in dimension. Fig. 1c shows high-magnification SEM images viewed from overhead, high dense alignment rod on the substrate are clearly observed. The density of SnO_2 grown nanorods is statistically counted to *ca.* 200-250 μm^{-2}. The insert in Fig. 1c is a cross-sectional SEM image of the regarded SnO_2 nanorods arrays. It shows that the SnO_2 nanorods have a diameter of ~ 50 nm. Fig. 1d viewed from laterally is present. It shows that SnO_2 nanorods grow on the two sides of the substrate, and the axial length of the nanorods is estimated to be in the range of 150 - 200 nm. Fig. 1e shows a low-magnification TEM image of an individual SnO_2 nanorod. The corresponding selected area electron diffraction (SAED) pattern (insert Fig. 1e) indicates that the SnO_2 nanorod is a single crystal structure and projected from the [$\bar{1}$10] zone axis. It also indicates that the growth direction of SnO_2 nanorod is parallel to [001] crystalline orientation. The HRTEM image of the SnO_2 nanorod edge in Fig. 1f shows that the crystal spacing is 0.345 nm corresponding well with the lattice fringes of {110} plane of the tetragonal rutile structure SnO_2 crystal. These results indicate that the exposed facets of the SnO_2 nanorods are {110} facets.

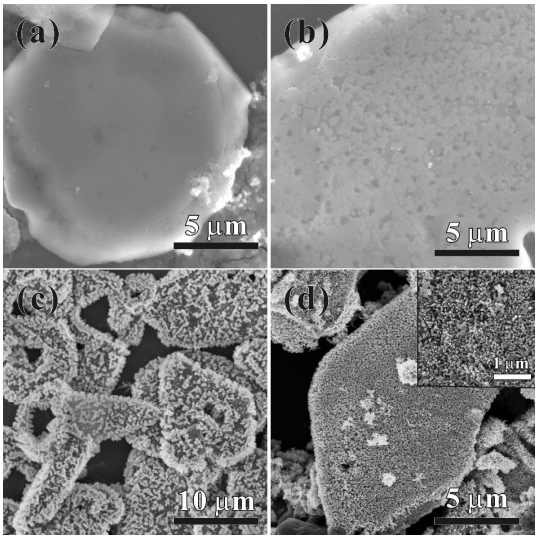

Fig. 2 Temporal evolution of SEM images of SN sample (a) 1 h, (b) 3 h, (c) 6 h, (d) 8 h.

In order to reveal the growth mechanism of the SN hierarchical structure, a serial of time-dependent experiments have been performed to observe the formation process of the product obtained by the hydrothermal process at 200 ^oC for different time. Fig. 2 shows the SEM images of intermediate products collected at 200 ^oC after 1, 3, 6 and 8 h, respectively. The corresponding XRD patterns are recorded (Fig. 3). The peaks marked by the frame are the rutile SnO_2 (110) reflection. When the reaction time is 1 h, a great deal of bulk crystals with smooth surface have been formed in a high yield (Fig. 2a). As shown in Fig. 3a, the majority of the diffraction peaks can be indexed to $Na_2Sn(OH)_6$, and the intensity of the SnO_2 peak is weak. Prolonging the reaction time to 3 h, the surface of the bulk become coarseness (Fig. 2b), the diffraction peaks of SnO_2 become relatively strong (Fig. 3b). Further extending of the reaction time to 6 h, interestingly, a large number of nanoparticles grow on the surface of bulk crystals (Fig. 2c). The diffraction peaks of rutile SnO_2 become further strong (Fig. 3c). When the reaction time prolong to 8h, the nanoparticles on the surface become vertical rods (Fig. 2d), the diffraction peaks of SnO_2 (110) reflection become stronger (Fig. 3d). These results indicate that the material of the substrates are $Na_2Sn(OH)_6$, and the vertical rods are rutile SnO_2. And the SnO_2 nanorods gradually grow long with prolonging the reaction time.

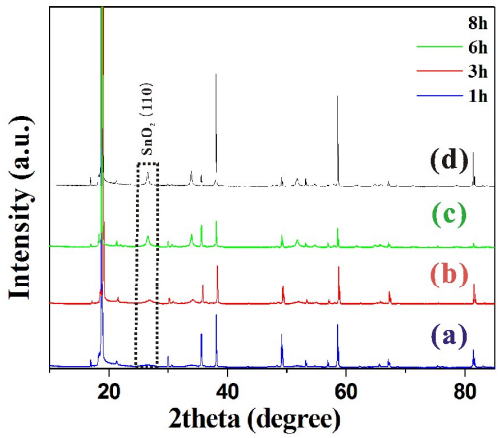

Fig. 3 Temporal evolution of XRD patterns of SN sample (a) 1 h, (b) 3 h, (c) 6 h, (d) 8 h.

On the basis of the above experimental results, a possible growth mechanism can be proposed, as shown schematically in scheme 1. In this formation process, time was the most important controlling factor. We speculate that the SN array structure are formed in three steps. In the initial stage, $SnCl_4$ reacts with NaOH to form $Na_2Sn(OH)_6$ in the water and ethanol environment with the assistant of PVP. With extension of the reaction time, the surface of $Na_2Sn(OH)_6$ decomposed to small particles of SnO_2 as the seeds. Due to the sustaining accumulation of SnO_2 seeds, the SnO_2 seeds on the $Na_2Sn(OH)_6$ substrate promote the occurrence of anisotropic growth and induce the formation of regular nanostructures. Because of the intrinsic anisotropic nature of rutile SnO_2, it tends to grow along the [001] zone axis and with a square cross-section. Therefore, the aligned SnO_2 rods on the $Na_2Sn(OH)_6$ substrate have been synthesized.

CrystEngComm Accepted Manuscript

This journal is © The Royal Society of Chemistry [year]

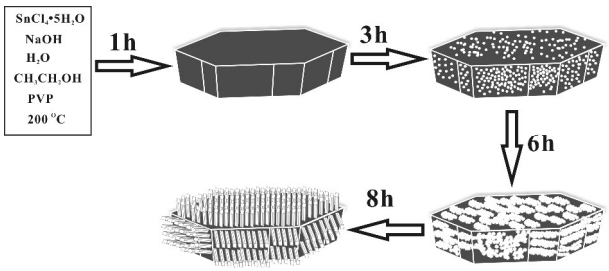

Scheme 1 Schematic illustration of the formation mechanism of SN arrayed hierarchical structure.

The products prepared at different reaction time are investigated by the electrochemical properties as lithium-ion batteries anode. Fig. 4 (a-e) respectively show the charge-discharge voltage profiles of the sample prepared at different time for the 1st , 10th, and 20th cycles at a current rate of 100 mA g^{-1} over the potential range of 0.1 V to 2.5 V. The first discharge and charge capacities are 1397 and 294 mAh g^{-1} for the sample prepared at 1 h, 1649 and 407 mAh g^{-1} for the sample prepared at 3 h, 1745 and 717 mAh g^{-1} for the sample prepared at 6 h, 1805 and 761 mAh g^{-1} for the sample prepared at 8 h, 1930 and 867 mAh g^{-1} for the sample prepared at 18 h. The theoretical energy capacity of SnO_2 is about 790 mAh g^{-1}, while the dates are highter than the theroretical energy capacity, which was ascribed to the formation of a solid electrolyte interface (SEI) layer due to the electrolyte decomposition on the electrode surface. The results indicate that the charge-dischrage capacity increased with prolonging the reaction time. Fig. 4f presents the cycling ability of the product prepared at different time. It also indicates that the cycling ability increases with the prolonging the reaction time, which could be attribute to the increasing density of SnO_2 arrays with prolonging reaction time, and then enhance the charge transport in SnO_2 arrays.

In summary, the highly aligned SnO_2 nanorods on self-produced $Na_2Sn(OH)_6$ substrate have been synthesized by one-step template-free hydrothermal synthesis method. The TEM images indicate that the SnO_2 nanorods were exposed with {110} facet. By changing the reaction time, we speculate that the SN array structure are formed in three steps. The first step is forming $Na_2Sn(OH)_6$ substance and then the $Na_2Sn(OH)_6$ substance decomposes to small SnO_2 particles. With prolonging the reaction time, the small SnO_2 particles gradually grow into SnO_2 nanorods arrays. The performance of lithium-ion batteries indicate that the charge-dischrage capacity and the cycling ability increase with the prolonging the reaction time.

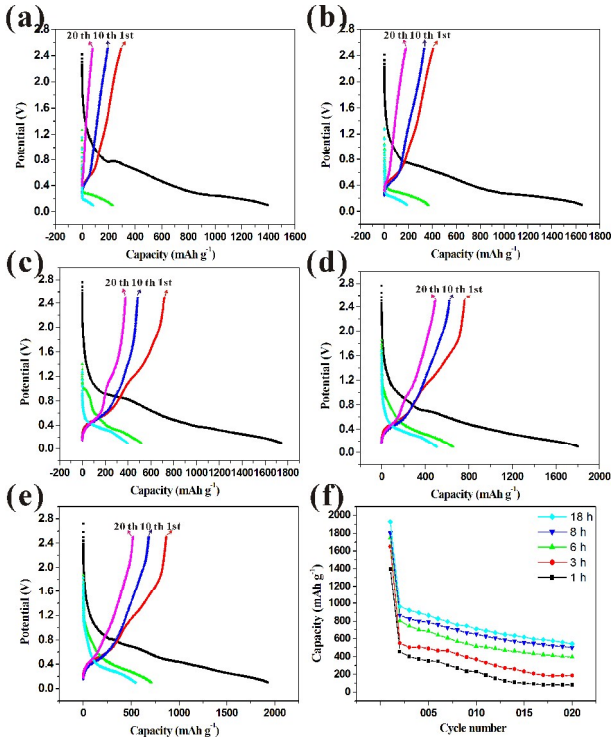

Fig. 4 The charge/discharge curves of samples prepared at different time (a) 1 h, (b) 3 h, (c) 6 h, (d) 8 h, (e) 18 h for the 1st, 10th and 20th cycle between at 0.1 and 2.5 V at a rate of 100 mA g^{-1}, (f) comparison of cycling performance of the samples prepared at different time.

This work was supported by the National Natural Science Foundation of China (Grant No. 21201088), the Qing Lan Project and the Project Funded by the Priority Academic Program Development of Jiangsu Higher Education Institutions.

Notes and references

[a] *Department of Chemistry, School of Chemistry and Chemical Engineering, Jiangsu Normal University, Xuzhou, 221116, P. R. China.*
[b] *Jiangsu Key Laboratory of Green Synthetic Chemistry for Functional Materials, Xuzhou, 221116, P. R. China.*
E-mail: xghan@jsnu.edu.cn

† Electronic Supplementary Information (ESI) available: the preparation and characterization of SN and measurement of lithium-ion batteries. See DOI:10.1039/b000000x/

1 M. Armand, J. M. Tarascon, *Nature,* **2008**, *451,* 652.
2 P. Simon, Y. Gogotsi, *Nat. Mater.,* **2008,** *7,* 845.
3 A. S. Arico, P. Bruce, B. Scrosati, J. M. Tarascon, W. Schalkwijk, *Nat. Mater.,* **2005,** *4,* 366.
4 N. Ravet, Y. Chouinard, J. F. Magnan, S. Besner, M. Gauthier, M. Armand, *J. Power Sources,* **2000,** *503,* 197.
5 Y. H. Ding, P. Zhang, Y. Jiang, D. S. Gao, *Solid State Ionics,* **2007,** *178,* 967.
6 M. Okubo, E. Hosono, T. Kudo, H. S. Zhou, I. Honma, *Solid State Ionics,* **2009,** *180,* 612.
7 K. T. Nam, D.W. Kim, P. J. Yoo, C.Y. Chiang, N. Meethong, P. T. Hammond, Y. M. Chiang, A. M. Belcher, *Science,* **2006,** *312,* 885.
8 C. M. Park, J. H. Kim, H. Kim, H. J. Sohn, *Chem. Soc. Rev.,* **2010,** *39,* 3115.
9 M. R. Palacin, *Chem. Soc. Rev.,* **2009,** *38,* 2565.
10 Y. Shi, B. Guo, S. A. Corr, Q. Shi, Y. S. Hu, K. R. Heier, L. Chen, R. Seshadri, G. D. Stucky, *Nano Lett.,* **2009,** *9,* 4215.
11 Y. Idota, T. Kubota, A. Matsufuji, Y. Maekawa, T. Miyasaka, *Science,* **1997,** *276,* 1395.
12 X. W. Lou, C. M. Li, L. A. Archer, *Adv. Mater.,* **2009,** *21,* 2536.

CrystEngComm Accepted Manuscript

13 S. Han, B. Jang, T. Kim, S. M. Oh, T. Hyeon, *Adv. Funct. Mater.,* **2005,** *15,* 1845.
14 M. S. Park, Y. M. Kang, G. X. Wang, S. X. Dou, H. K. Liu, *Adv. Funct. Mater.,* **2008,** *18,* 455.
15 M. Wachtler, M. Winter, J. O. Besenhard, *J. Power Sources,* **2002,** *105,* 151.
16 B. A. Boukamp, G. C. Lesh, R. A. Huggins, *J. Electrochem. Soc.,* **1981,** *128,* 725.
17 Y. S. Hu, D. C. Rezan, M. M. Titirici, J. O. Muller, R. Schlogl, M. Antonietti, J. Maier, *Angew. Chem., Int. Ed.,* **2008,** *47,* 1645.
18 G. Chen, Z. Wang, D. Xia, *Chem. Mater.,* **2008,** *20,* 6951.
19 S. Gubbala, V. Chakrapani, V. Kumar, M. K. Sunkara, *Adv. Funct. Mater.,* **2008,** *18,* 2411.
20 Y. Wang, J. Y. Lee, H. C. Zeng, *Chem. Mater.,* **2005,** *17,* 3899.
21 Z. Y. Wang, D. Y. Luan, F. Y. C. Boey, X. W. Lou, *J. Am. Chem. Soc.,* **2011,** *133,* 4738.
22 X. Wang, H. Guan, S. Chen, H. Li, T. Zhai, D. Tang, Y. Bando, D. Golberg, *Chem. Commun.,* **2011,** *47,* 12280.
23 D. Lei, M. Zhang, B. Qu, L. Chen, Y. Wang, E. Zhang, Z. Xu, Q. Li, T. Wang, *Nanoscale,* **2012,** *4,* 3422.
24 J. Liu, Y. C. Zhou, C. P. Liu, J. B. Wang, Y. Pan, D. Xue, *CrystEngComm,* **2012,** *14,* 2669.
25 J. Jiang, Y. Y. Li, J. P. Liu, X. T. Huang, C. Z. Yuan, X. W. Lou, *Adv. Mater.,* **2012,** *24,* 5166.
26 S. C. Zhang, Z. J. Du, R. X. Lin, T. Jiang, G. R. Liu, X. M. Wu D. S. Weng, *Adv. Mater.,* **2010,** *22,* 5378.
27 F. F. Cao, J. W. Deng, S. Xin, H. X. Ji, O. G. Schmidt, L. J. Wan, Y. G. Guo, *Adv. Mater.,* **2011,** *23,* 4415.
28 J. P. Liu, Y. Y. Li, X. T. Huang, R. M. Ding, Y. Y. Hu, J. Jiang, L. Liao, *J. Mater. Chem.,* **2009,** *19,* 1859.
29 S. Chen, M. Wang, J. F. Ye, J. G. Cai, Y. R. Ma, H. H. Zhou, L. M. Qi, *Mater. Today,* **2012,** *15,* 246.
30 J. Zhu, D. N. Lei, G. H. Zhang, Q. H. Li, B. G. Lu, T. H. Wang, *Nanoscale*, **2013**, *5*, 5499.
31 D. N. Wang, J .L. Yang, X. F. Li, D. S. Geng, R. Y. Li, M. Cai, T. K Sham, X. L. Sun, *Energy Environ. Sci.,* **2013,** *6,* 2900.
32 Q. Y. Han, J. T. Zai, Y. L. Xiao, B. Li, M. Xu, X. F. Qian, *RSC Adv.,* **2013,** *3*, 20573.
33 Y. Liu, J. Dong, M.L. Liu, *Adv. Mater.,* **2004,** *16,* 353.
34 Y. Liu, M. L. Liu, *Adv. Funct. Mater.,* **2005,** *15,* 57.
35 H. Huang, O. K. Tan, Y. C. Lee, T. D. Tran, M. S. Tse, *Appl. Phys. Lett.,* **2005,** *87,* 163123.
36 L. Vayssieres, *Angew. Chem. Int. Ed.,* **2004,** *43,* 3666.
37 L. A. Ma, *Physica B,* **2008,** *403,* 3410.
38 G. Cheng, K. Wu, P. Zhao, Y. Cheng, X. He, K. Huang, *J. Cryst. Growth,* **2007,** *309,* 53.
39 M. Zheng, G. Li, X. Zhang, S. Huang, Y. Lei, L. Zhang, *Chem. Mater.,* **2001,** *13,* 3859.
40 K. H. Wu, S. Y. Lu, *Electrochem. Solid-State Lett.,* **2005,** *8,* D9.
41 Y. L. Wang, M. Guo, M. Zhang, X. D. Wang, *Thin Solid Films,* **2010,** *518,* 5098.
42 X. Y. Xue, S. Yuan, L. L. Xing, Z. H. Chen, B. Hea, Y. J. Chen, *Chem. Commun.,* **2011,** *47,* 4718.

CrystEngComm Accepted Manuscript

This journal is © The Royal Society of Chemistry [year]

Graphical Abstract

The highly aligned SnO_2 nanorods on self-produced $Na_2Sn(OH)_6$ substrate have been synthesized and exhibit high-performance of Li-ion battery.

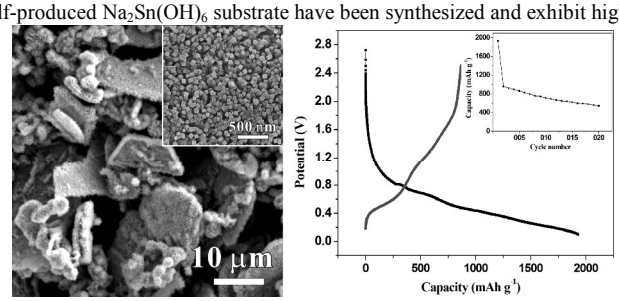

CrystEngComm Accepted Manuscript